

INVESTIGATIONS OF PRECISE FUNCTION APPROXIMATION FOR THE FORCE OF FLUIDIC MUSCLE IN MS EXCEL

József Sárosi¹ – Zoltán Fabulya² – Gábor Szabó³ – Péter Szendrő⁴

¹Technical Department, Faculty of Engineering
University of Szeged, H-6724 Szeged, Mars tér 7, Hungary
e-mail: sarosi@mk.u-szeged.hu

²Economics and Rural Development Department, Faculty of Engineering
University of Szeged, H-6724 Szeged, Mars tér 7, Hungary
e-mail: fabulya@mk.u-szeged.hu

³Department of Process Engineering, Faculty of Engineering
University of Szeged, H-6724 Szeged, Mars tér 7, Hungary
e-mail: szabog@mk.u-szeged.hu

⁴Institute of Mechanics and Machinery, Faculty of Mechanical Engineering
Szent István University, H-2103 Gödöllő, Páter K. u. 1, Hungary
e-mail: szendro.peter@gek.szie.hu

ABSTRACT

The newest and most promising type of pneumatic actuators is the pneumatic artificial muscle (PAM). Different designs have been developed, but the McKibben muscle is the most popular and is made commercially available by different companies (e. g. Fluidic Muscle manufactured by Festo Company). The most often mentioned characteristic of PAMs is the force as a function of pressure and contraction. In this paper our newest function approximation for the force generated by Fluidic Muscles is shown that can be generally used for different muscles made by Festo Company.

1. INTRODUCTION

Pneumatic artificial muscle is a membrane that will expand radially and contract axially when inflated, while generating high pulling force along the longitudinal axis. PAMs have different names in literature: Pneumatic Muscle Actuator, Fluid Actuator, Fluid-Driven Tension Actuator, Axially Contractible Actuator, Tension Actuator, etc. ([1] and [2]).

The working principle of pneumatic muscles is well described in [1], [2], [3], [4] and [5].

There are a lot of advantages of PAMs like the high strength, good power-weight ratio, low price, little maintenance needed, great compliance, compactness, inherent safety and usage in rough environments ([4] and [6]). The main disadvantage of these muscles is that their dynamic behaviour is highly nonlinear ([4], [7], [8], [9], [10] and [11]).

Many researchers have investigated the relationship of the force, length and pressure to find a good theoretical approach for the equation of force produced by pneumatic artificial muscles. Some of them report several mathematical models, but significant differences have been noticed between the theoretical and experimental results ([4], [6], [12], [13], [14] and [15]).

The force depends on length (contraction) under constant pressure. This force decreases with increasing position of the muscle and the muscle inflates. Our goal was to develop a precise approximation algorithm with minimum numbers of parameters for the force of different Fluidic Muscles.

The layout of this paper is as follows. Section 2 (Materials and Methods) presents the static modelling of PAMs and several force equations. Section 3 (Results and Discussion) compares the measured and calculated data. Finally, Section 4 (Conclusion and Future Work) gives the investigations we plan.

Fluidic Muscles type DMSP-20-400N-RM-RM (with inner diameter of 20 mm and initial length of 400 mm) produced by Festo Company was selected for our newest study (Figure 1).



Figure 1. Festo Fluidic Muscle

2. MATERIALS AND METHODS

The general behaviour of PAMs with regard to shape, contraction and tensile force when inflated depends on the geometry of the inner elastic part and of the braid at rest (Figure 2), and on the materials used [1]. Typical materials used for the membrane construction are latex and silicone rubber, while nylon is normally used in the fibres.

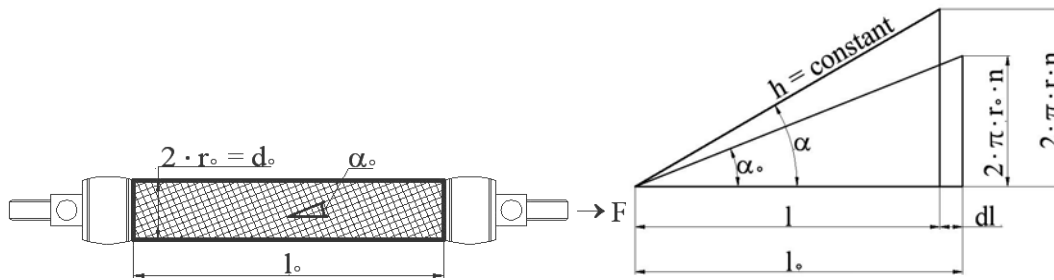


Figure 2. Geometry parameters of PAMs

With the help of [4] and [6], the input and output (virtual) work can be calculated:

$$dW_{in} = p \cdot dV \quad (1)$$

dW_{in} can be divided into a radial and an axial component:

$$dW_{in} = 2 \cdot r \cdot \pi \cdot p \cdot l \cdot (+dr) - r^2 \cdot \pi \cdot p \cdot (-dl) \quad (2)$$

The output work:

$$dW_{out} = -F \cdot dl \quad (3)$$

By equating the virtual work components:

$$dW_{in} = dW_{out} \quad (4)$$

Using (1) and (3):

$$F = -p \cdot \frac{dV}{dl} \quad (5)$$

Using (2) and (3):

$$F = -2 \cdot r \cdot \pi \cdot p \cdot l \cdot \frac{dr}{dl} - r^2 \cdot \pi \cdot p \quad (6)$$

On the basis of Figure 2:

$$\cos \alpha_0 = \frac{l_0}{h} \text{ and } \cos \alpha = \frac{l}{h} \quad (7)$$

$$\sin \alpha_0 = \frac{2 \cdot \pi \cdot r_0 \cdot n}{h} \text{ and } \sin \alpha = \frac{2 \cdot \pi \cdot r \cdot n}{h} \quad (8)$$

$$\frac{l}{l_0} = \frac{\cos \alpha}{\cos \alpha_0} \text{ and } \frac{r}{r_0} = \frac{\sin \alpha}{\sin \alpha_0} \quad (9)$$

$$r = r_0 \cdot \frac{\sqrt{1 - \cos^2 \alpha}}{\sin \alpha_0} = r_0 \cdot \frac{\sqrt{1 - \left(\frac{l}{l_0} \cdot \cos \alpha_0 \right)^2}}{\sin \alpha_0} \quad (10)$$

$$\frac{dr}{dl} = - \frac{r_0 \cdot l \cdot \cos^2 \alpha_0}{l_0^2 \cdot \sin \alpha_0} \cdot \frac{1}{\sqrt{1 - \left(\frac{l}{l_0} \cdot \cos \alpha_0 \right)^2}} \quad (11)$$

By using (10) and (11) with (6) the force equation is found:

$$F(p, \kappa) = r_0^2 \cdot \pi \cdot p \cdot (a \cdot (1 - \kappa)^2 - b) \quad (12)$$

Where $a = \frac{3}{\text{tg}^2 \alpha_0}$, $b = \frac{1}{\sin^2 \alpha_0}$, $\kappa = \frac{l_0 - l}{l_0}$, $0 \leq \kappa \leq \kappa_{\max}$, and V the muscle volume, F the pulling force, p the applied pressure, r_0 , l_0 , α_0 the initial inner radius and length of the PAM and the initial angle between the thread and the muscle long axis, r , l , α the inner radius and length of the PAM and angle between the thread and the muscle long axis when the muscle is contracted, h the constant thread length, n the number of turns of thread and κ the contraction.

Consequently:

$$F_{\max} = r_0^2 \cdot \pi \cdot p \cdot (a - b), \text{ if } \kappa = 0 \quad (13)$$

and

$$\kappa_{\max} = 1 - \sqrt{\frac{b}{a}}, \text{ if } F = 0 \quad (14)$$

Equation (12) is based on the admittance of a continuously cylindrical-shaped muscle. The fact is that the shape of the muscle is not cylindrical on the end, but rather is flattened, accordingly, the more the muscle contracts, the more its active part decreases, so the actual maximum contraction ration is smaller than expected [4].

Tondu and Lopez in [4] consider improving (12) with a correction factor ε , because it predicts for various pressures the same maximal contraction. This new equation is relatively good for higher pressure ($p \geq 200$ kPa). Kerscher et al. in [13] suggest achieving similar approximation for smaller pressure another correction factor μ is needed, so the modified equation is:

$$F(p, \kappa) = \mu \cdot r_0^2 \cdot \pi \cdot p \cdot (a \cdot (1 - \varepsilon \cdot \kappa)^2 - b) \quad (15)$$

Where $\varepsilon = a_\varepsilon \cdot e^{-p} - b_\varepsilon$ and $\mu = a_\mu \cdot e^{-\kappa \cdot 40} - b_\mu$.

We noticed significant differences between the theoretical and experimental results, therefore we have introduced a new approximation algorithm:

$$F(p, \kappa) = (a \cdot p + b) \cdot e^{(c \cdot \kappa + d)} + (e \cdot p + f) \cdot \kappa + g \cdot p + h \quad (16)$$

Beforehand the unknown parameters of (16) were found using genetic algorithm in Matlab ([16] and [17]).

With reduced number of parameters the force can be calculated:

$$F(p, \kappa) = (a \cdot p + b) \cdot e^{c \cdot \kappa} + d \cdot p \cdot \kappa + e \cdot p + f \quad (17)$$

On the basis of our investigations and results, (17) can be simplified:

$$F(p, \kappa) = (p + a) \cdot e^{b \cdot \kappa} + c \cdot p \cdot \kappa + d \cdot p + e \quad (18)$$

In this work the unknown parameters of (17) and (18) were found in MS Excel instead of Matlab.

3. RESULTS AND DISCUSSION

Our newest analyses were carried out in MS Excel. Tensile force of Fluidic Muscle under different constant pressures is a function of muscle length (contraction). The force always drops from its highest value at full muscle length to zero at full inflation and position (Figure 3).

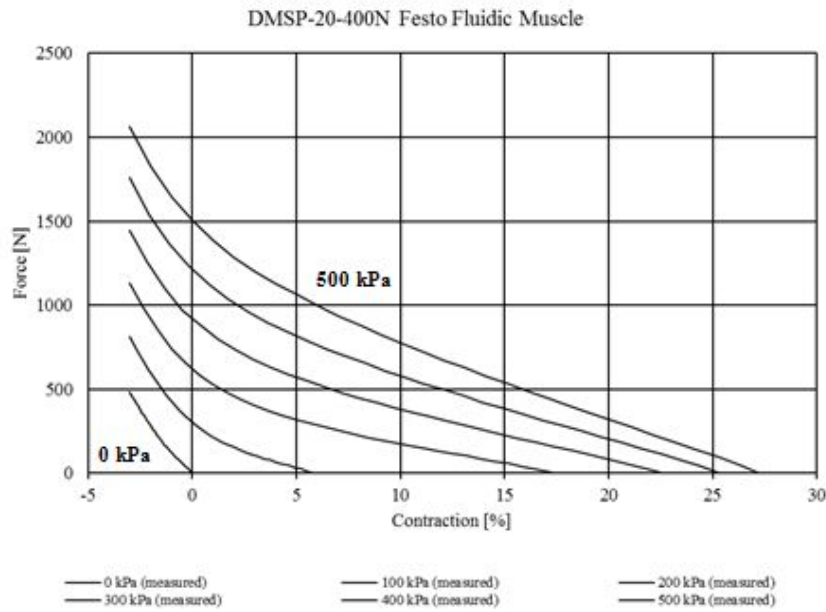


Figure 3. Isobaric force-contraction diagram

Firstly, the measured data and (12) was compared. As it is shown in Figure 4, there is only one intersection point between the measured and calculated results and no fitting.

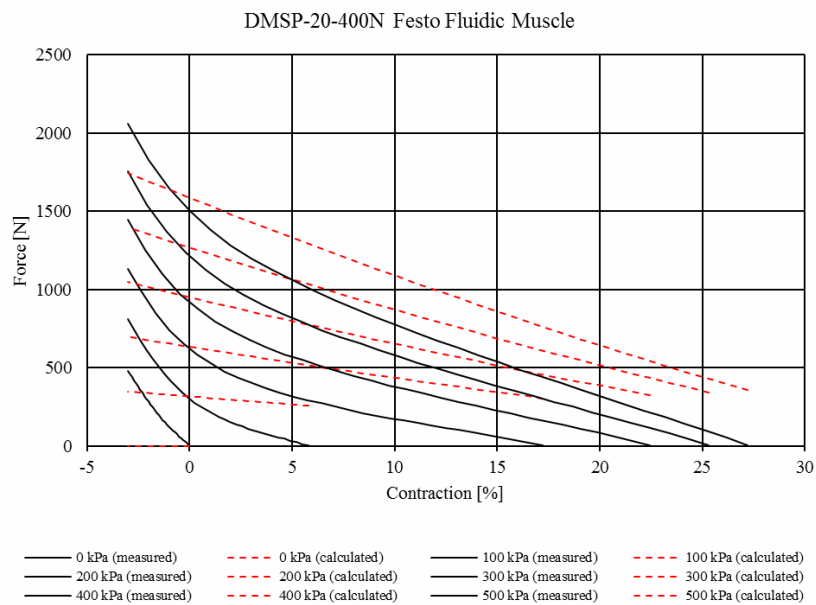


Figure 4. Comparison of measured data and (12)

In the interest of fitting we repeated the simulation with (15) (Figure 5). The coefficients (a_ϵ , b_ϵ , a_κ and b_κ) of (15) were found using Solver in MS Excel. Values of unknown parameters of (15) are listed in Table 1.

Table 1. Values of unknown parameters of (15)

Parameters	Values
a_ϵ	0,076042885
b_ϵ	-0,502357905
a_κ	9,74938E+28
b_κ	-2,801103661

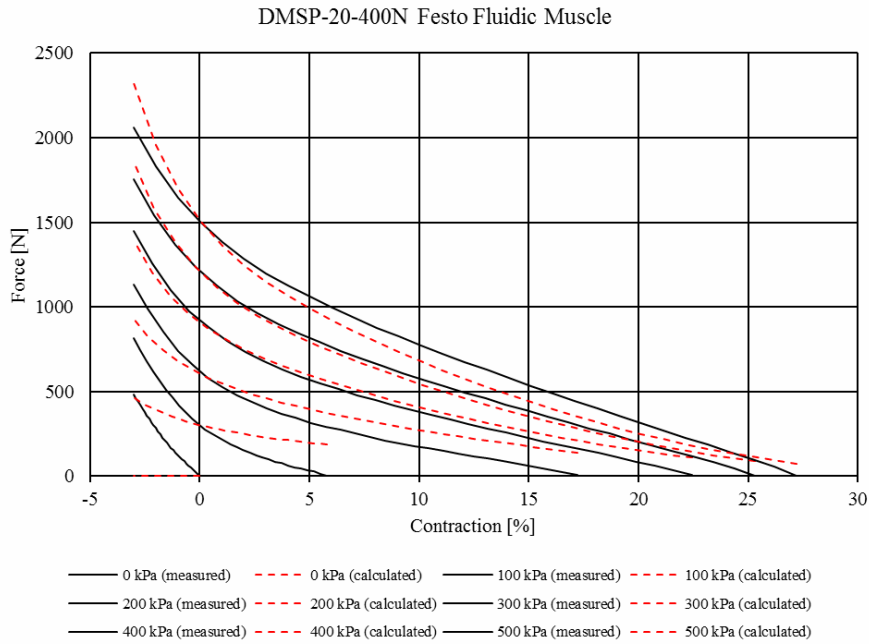


Figure 5. Comparison of measured data and (15)

Figure 5 shows the measured and calculated results still do not fit. Better fitting was attained, but at a pressure of 0 Bar we still have a rather substantial inconsistency.

To improve fitting quality under different pressures including 0 Bar we have introduced new approximation algorithms with 6 and 5 parameters. The unknown parameters of (17) and (18) can be found using Solver in MS Excel, too. Values of these unknown parameters are shown in Table 2. and Table 3.

Table 2. Values of unknown parameters of (17)

Parameters	Values
a	-4,76857022
b	283,8967156
c	-0,32748087
d	-9,26394297
e	302,9755164
f	-267,407845

Table 3. Values of unknown parameters of (18)

Parameters	Values
a	277,6596545
b	-0,32451181
c	-9,04546346
d	296,760048
e	-258,037076

The accurate fitting of (17) and (18) can be seen in Figure 6 and Figure 7.

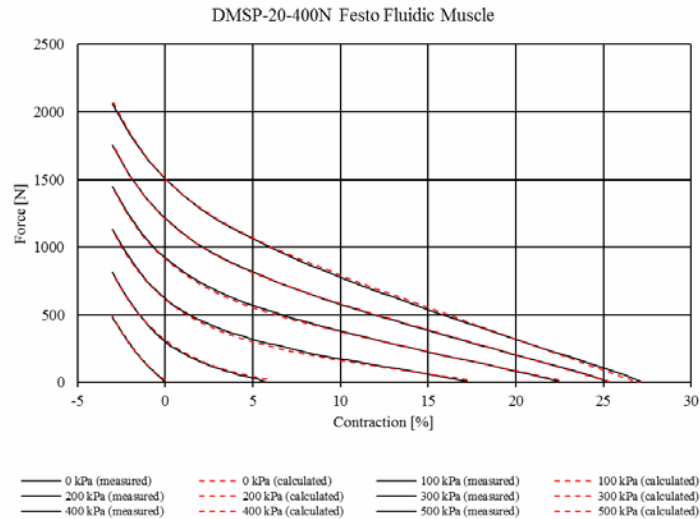


Figure 6. Comparison of measured data and (17)

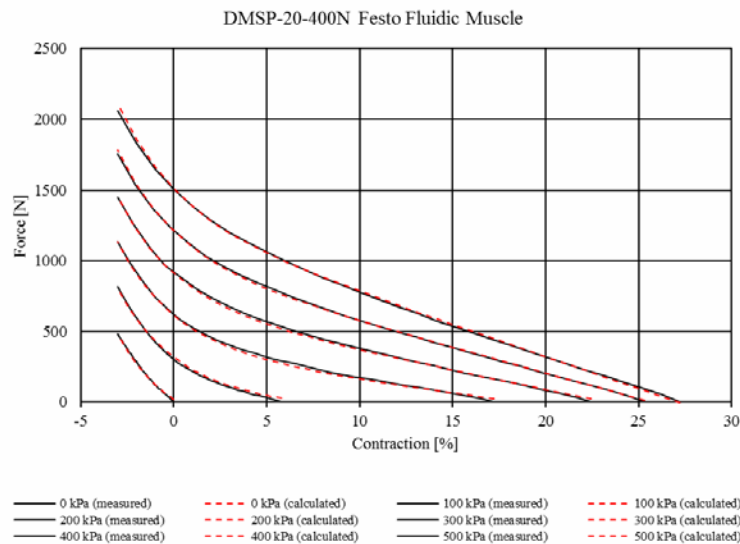


Figure 7. Comparison of measured data and (18)

As we can see we have consistent fitting even at a pressure of 0 Bar.

4. CONCLUSION AND FUTURE WORK

In this work new functions for the force produced by Festo Fluidic Muscle have been introduced. The accuracy of fitting has been proved with comparisons of the measured and calculated data. These investigations were carried out in MS Excel instead of Matlab. This environment and solution is more favourable, because programming is not required. Our main aim is to develop a new general mathematical model for pneumatic artificial muscles on the basis of our new models and results.

REFERENCES

1. Daerden, F. (1999): Conception and Realization of Pleated Artificial Muscles and Their Use as Compliant Actuation Elements. PhD Dissertation, Vrije Universiteit Brussel, Faculteit Toegepaste Wetenschappen Vakgroep Werktuigkunde, 5-24 p.

2. Daerden, F., Lefeber, D. (2002): Pneumatic Artificial Muscles: Actuator for Robotics and Automation. *European Journal of Mechanical and Environmental Engineering*, 2002:47, 10-21 p.
3. Caldwell, D. G., Razak, A., Goodwin, M. J. (1993): Braided Pneumatic Muscle Actuators. *Proceedings of the IFAC Conference on Intelligent Autonomous Vehicles*, Southampton, United Kingdom, 18-21 April, 1993, 507-512 p.
4. Tondu, B., Lopez, P. (2000): Modelling and Control of McKibben Artificial Muscle Robot Actuator. *IEEE Control System Magazine*, 2000:20, 15-38 p.
5. Balara, M., Petík, A. (2004): The Properties of the Actuators with Pneumatic Artificial Muscles. *Journal of Cybernetics and Informatics*, 2004:4, 1-15 p.
6. Chou, C. P., Hannaford, B. (1996): Measurement and Modeling of McKibben Pneumatic Artificial Muscles. *IEEE Transactions on Robotics and Automation*, 1996:12 (1), 90-102 p.
7. Caldwell, D. G., Medrano-Cerda, G. A., Goodwin M. (1995): Control of Pneumatic Muscle Actuators. *IEEE Control System Magazine*, 1995:15 (1), 40-48 p.
8. Lamár, K. (2004): Inaccuracies in Digitally Controlled Induction Motor Drives. 21st Joint Scientific Conference „Science for Practice”, Subotica, Serbia, 4-6 May, 2004, 33-41 p.
9. Tian, S., Ding, G., Yan, D., Lin, L., Shi, M. (2004): Nonlinear Controlling of Artificial Muscle System with Neural Networks. *International Conference on Robotics and Biomimetics*, Shenyang, China, 22-26 August, 2004, 56-59 p.
10. Udawatta, L., Priyadarshana, P., Witharana, S. (2007): Control of Pneumatic Artificial Muscle for Bicep Configuration using IBC, *Third International Conference on Information and Automation for Sustainability*, Melbourne, VIC, Australia, 4-6 December, 2007, 35-39 p.
11. Situm, Z., Herceg, Z. (2008): Design and Control of a Manipulator Arm Driven by Pneumatic Muscle Actuators. *16th Mediterranean Conference on Control and Automation*, Ajaccio, France, 25-27 June, 2008, 926-931 p.
12. Yee, N., Coghill, G. (2002): Modelling of a Novel Rotary Pneumatic Muscle, *Australasian Conference on Robotics and Automation*, Auckland, New Zealand, 27-29 November, 2002, 186-190 p.
13. Kerscher, T., Albiez, J., Zöllner, J. M., Dillmann, R. (2005): FLUMUT - Dynamic Modelling of Fluidic Muscles using Quick-Release, *3rd International Symposium on Adaptive Motion in Animals and Machines*, Ilmenau, Germany, 25-30 September, 2005, 1-6 p.
14. Ramasamy, R., Juhari, M. R., Mamat, M. R., Yaacob, S., Mohd Nasir, N. F., Sugisaka, M. (2005): An Application of Finite Element Modeling to Pneumatic Artificial Muscle, *American Journal of Applied Sciences*, 2005:2 (11), 1504-1508 p.
15. Borzikova, J., Balara, M., Pitel, J. (2007): The Mathematical Model of Contraction Characteristic $k = (F, p)$ of the Pneumatic Artificial Muscle, *XXXII. Seminar ASR '2007 "Instruments and Control"*, Farana, Smutný, Kočí & Babiuch, Ostrava, 2007, 21-25 p.
16. Sárosi, J., Szépe, T., Gyeviki, J. (2010): Approximation Algorithm for the Force of Pneumatic Artificial Muscles, *Factory Automation 2010*, Kecskemét, Hungary, 15-16 April, 2010, 101-104 p.
17. Sárosi, J., Szabó, G., Gyeviki, J. (2010): Investigation and Application of Pneumatic Artificial Muscles, *Biomechanica Hungarica*, 2010:3 (1), 208-214 p.